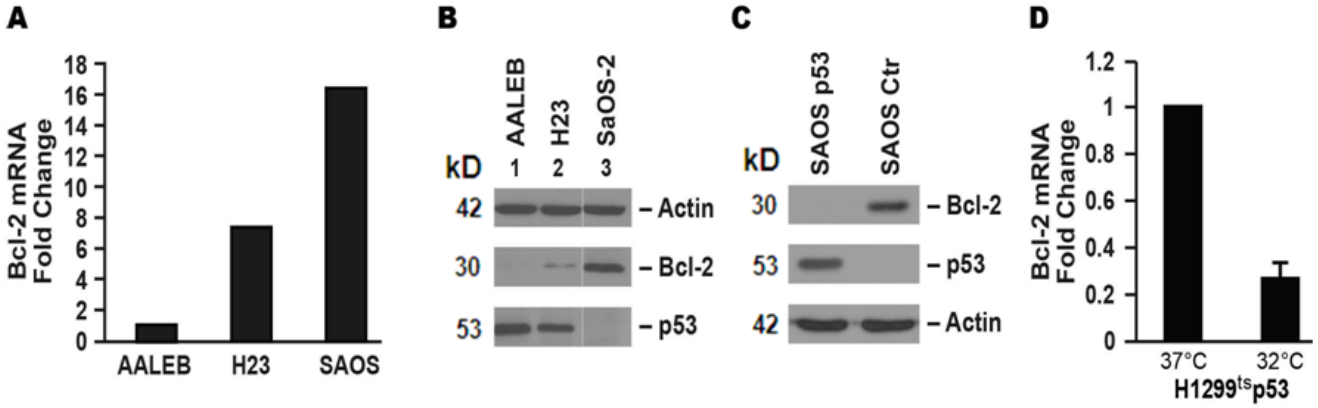

Supplementary Figure 1: (A) *Bcl-2* mRNA levels are inversely correlated with p53 protein levels. Total RNA was isolated from p53-expressing (AALEB and H23) and p53-deficient (SAOS-2) cell lines and *bcl-2* mRNA detected by qRT-PCR. RNA levels are expressed as fold change from levels found in AALEB cells. **(B)** Inverse relationship of p53 and Bcl-2 protein levels shown by Western blot analysis of AALEB, H23, and SAOS-2 cells. **(C)** Inverse relationship of p53 and Bcl-2 protein levels in SAOS-2 cells stably transfected with p53 (SAOS p53) and control vector (SAOS Ctr) analyzed by Western blotting. **(D)** *Bcl-2* mRNA levels are reduced in H1299 cells stably transfected with temperature-sensitive p53 (H1299p53^{ts} cells) when p53 is activated at 32°C. Bars = group means ± standard error from the mean (n = 3 different treatments/group).

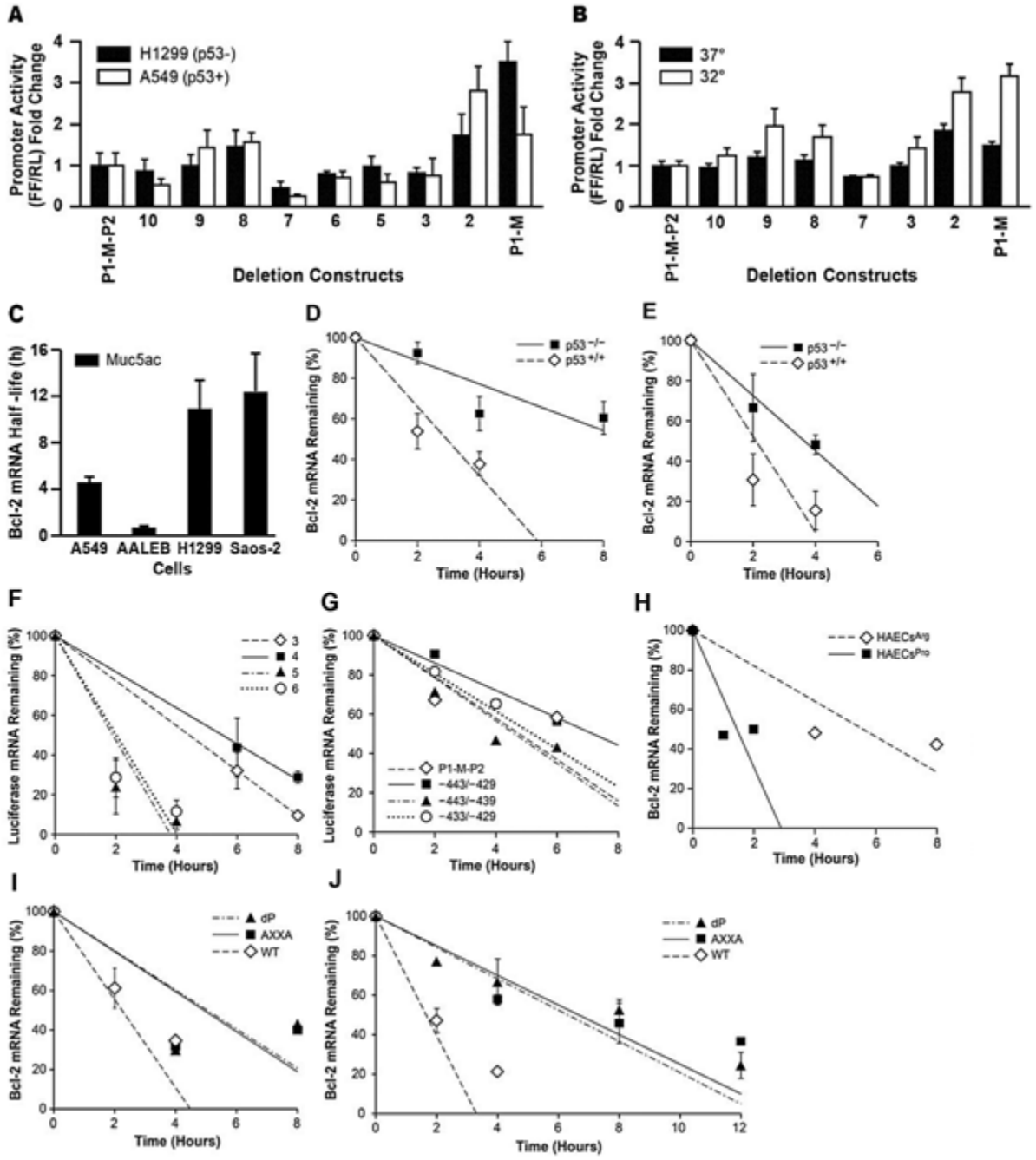

Supplementary Figure 2: p53 suppresses Bcl-2 expression independently of P2 by reducing *bcl-2* mRNA stability. (A) Analysis of P2-dependent suppression of P1-M-P2 promoter activity by using p53-sufficient (A549) and -deficient (H1299) cells. The activities of the full length P1-M-P2 and the derived constructs containing serially shorter P2 promoter regions (P1-M #s 10–2) (see Table 1 in supplementary information) were analyzed. Firefly/Renilla luciferase activities of the deletion constructs were normalized to the full-length construct. **(B)** H1299p53^{ts} cells were transfected with the full-length P1-M-P2 and the derived constructs containing serially shorter P2 promoter regions (P1-M #s 10–2). **(C)** p53 sufficient (A549 and AALEB) and p53 deficient (H1299 and SAOS-2) cells were treated with 50ng/ml DRB and RNA isolated at 0, 2, 4, 8, 12, 24 h. *Bcl-2* mRNA half-life was analyzed by qRT-PCR and normalized using 18SrRNA. **(D)** Decay curve for Fig. S2B. **(E)** Decay curve for Fig. 2E. **(F)** Decay curve for Fig. 2G. **(G)** Decay curve for Fig. 2J. **(H)** Decay curve for Fig. 3B. **(I)** Decay curve for Fig. 5B. **(J)** Decay curve for Fig. 5E. Bars = group means ± standard error from the mean (n = 3 different treatments/group).

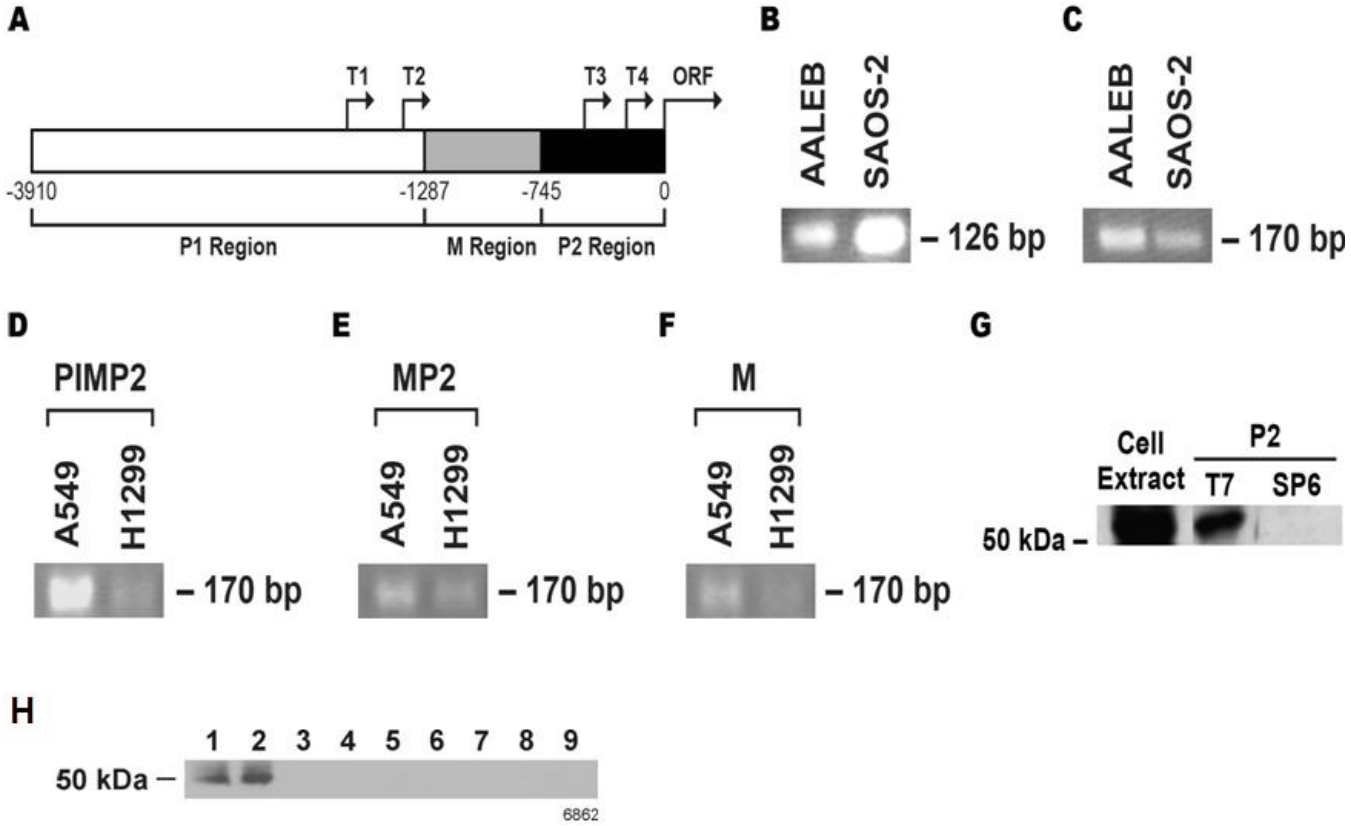

Supplementary Figure 3: The P2 and M regions are part of the 5'UTR of Bcl-2 mRNA. (A) Graphical representation of the transcriptional start sites within the 5'UTR region of the *bcl-2* mRNA. The 5'UTR of the *bcl-2* gene that is upstream of the TATA box was characterized by 5'RACE in primary normal human airway epithelial cells (HAECs). The P2 **(B)** and M **(C)** sequences are part of the 5'UTR. They were identified in DNase-treated mRNA isolated from p53 sufficient (A549) and p53 deficient (SAOS-2) cells by RT-PCR using primers specific to these regions. The M region was also detected by RT-PCR in DNase-treated mRNA isolated from A549 and H1299 cells transfected with either the full-length P1-M-P2 **(D)**, or the M-P2 **(E)**, or M **(F)** -promoter luciferase constructs using primers specific to M and the luciferase sequences. **(G)** The P2 region cloned in the pCRII dual promoter vector was used to generate Bio-11-UTP-labeled sense and anti-sense RNA using the T7 and Sp6 promoters, respectively; the labeled RNAs were used in pull-down assays using S-100 cytosolic extracts prepared from H1299p53^{ts} cells. p53 was detected in protein extract (lane 1), and in pull-down products using sense (lane 2) but not anti-sense RNA (lane 3). **(H)** Sense RNA products containing either the entire P2 region (lane 1) or only the 16 nucleotide (-443/-429) region of *bcl-2* mRNA pull down p53 (lane 2), but 4 nucleotide purine to pyrimidine substitutions (lanes 3, 4, 5, and 6) or 8 nucleotide substitutions (lanes 7 and 8) over the entire 16-nucleotide region abrogate the interaction with p53. Antisense mRNA synthesized from 16-nucleotide region upstream of (-608/-582) showed no interaction with p53 (lane 9).

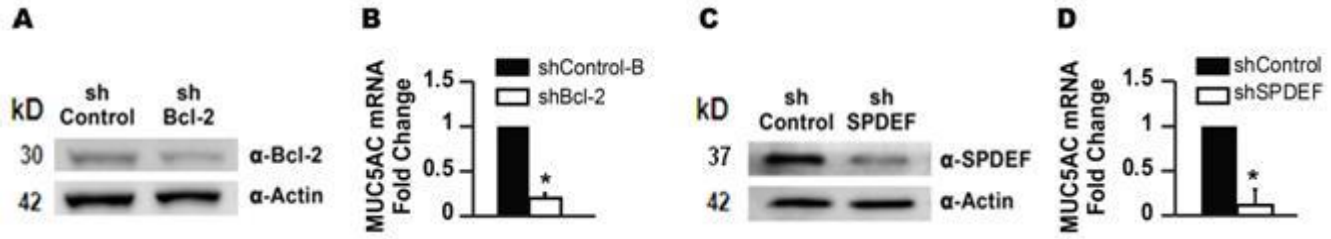

Supplementary Figure 4: Suppression of Bcl-2 or SPDEF reduces mucin differentiation. HAECs were differentiated on air-liquid interface cultures and infected with retroviral vectors expressing shBcl-2 or empty control **(A, B)** or shSPDEF or shControl **(C, D)**. Western blot analysis showing reduced Bcl-2 **(A)** and SPDEF **(C)** protein levels in cells infected with shBcl-2 or shSPDEF compared with shCtrl. Expression of β-actin was used as loading control. MUC5AC mRNA levels were reduced when these cells were infected with shBcl-2 **(B)** and shSPDEF **(D)** when compared to shControl. RNA was isolated from the same membrane that was used to harvest protein and analyzed by qRT-PCR. Bars = group means ± standard error from the mean (n = 3 different treatments/group); * *P*<0.05.

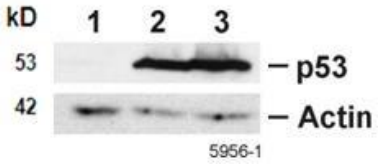

Supplementary Figure 5: Establishing cell lines with the Arg72 substitution by Pro72. The H1299 cell line, a p53-deficient cell line that is derived from a non-small cell lung cancer, was used to generate stable cell lines by transfecting with pCMV-neo-bam tsp53^{Arg72} or pCMV-neo-bam tsp53^{Pro72} plasmids (gift from Dr. Murphy, University of Pennsylvania, PA) that express temperature-sensitive p53 variants. These variants are essentially inactive at 37°C but are activated when cells are shifted to 32°C. Western blot analysis of extracts from H1299 (lane 1), H1299p53^{ts}Arg (lane 2) and H1299p53^{ts}Pro (lane 3) cells. Clones expressing similar p53 protein levels were selected for all experiments.

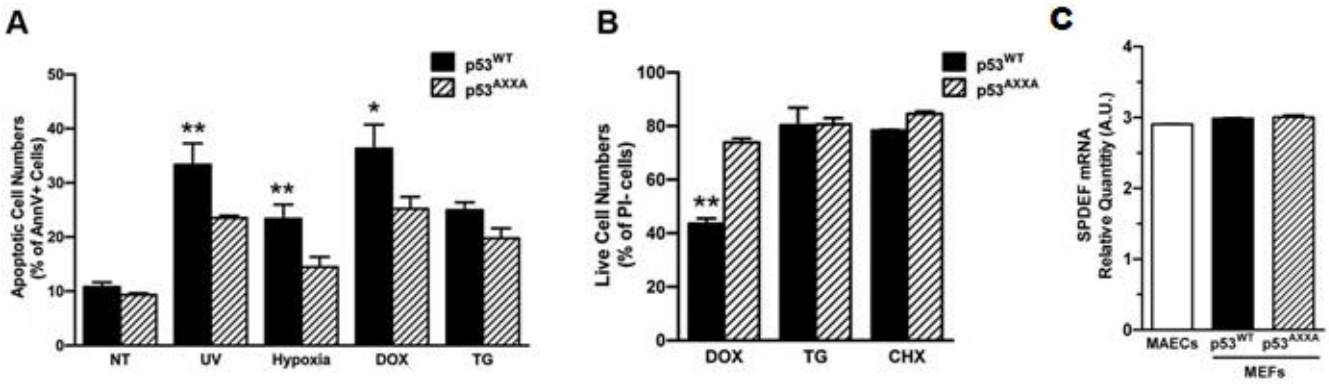

Supplementary Figure 6: The proline-rich domain of p53 affects DNA damage-induced cell death in MEFs. Comparison of cell death in $p53^{WT}$ and $p53^{AXXA}$ MEFs induced by DNA damage-inducing agents, UV-irradiation, hypoxia, doxorubicin, thapsigargin, and cyclohexamide. No differences were observed in thapsigargin- or cyclohexamide-induced cell death in MEFs from wild-type and $p53^{AXXA}$ mice. **(A)** MEFs were irradiated with 10 mJ UV, maintained in 2% O_2, treated with 1 μM doxorubicin, 10 μM cyclohexamide, or 1 μM thapsigargin for 18 h and analyzed by flow-cytometry for Annexin V and propidium iodide positivity. **(B)** MEFs were treated with 1 μM doxorubicin, 10 μM cyclohexamide, or 1 μM thapsigargin for 18 h and viable cell numbers were counted after trypan blue staining. **(C)** Relative quantity of SPDEF mRNA in MEFs from $p53^{WT}$ and $p53^{AXXA}$ mice compared to wild-type MAECs. Bars = group means ± standard error from the mean (n = 3 different treatments/group); * $P<0.05$; ** $P<0.01$.

Fig 2 C

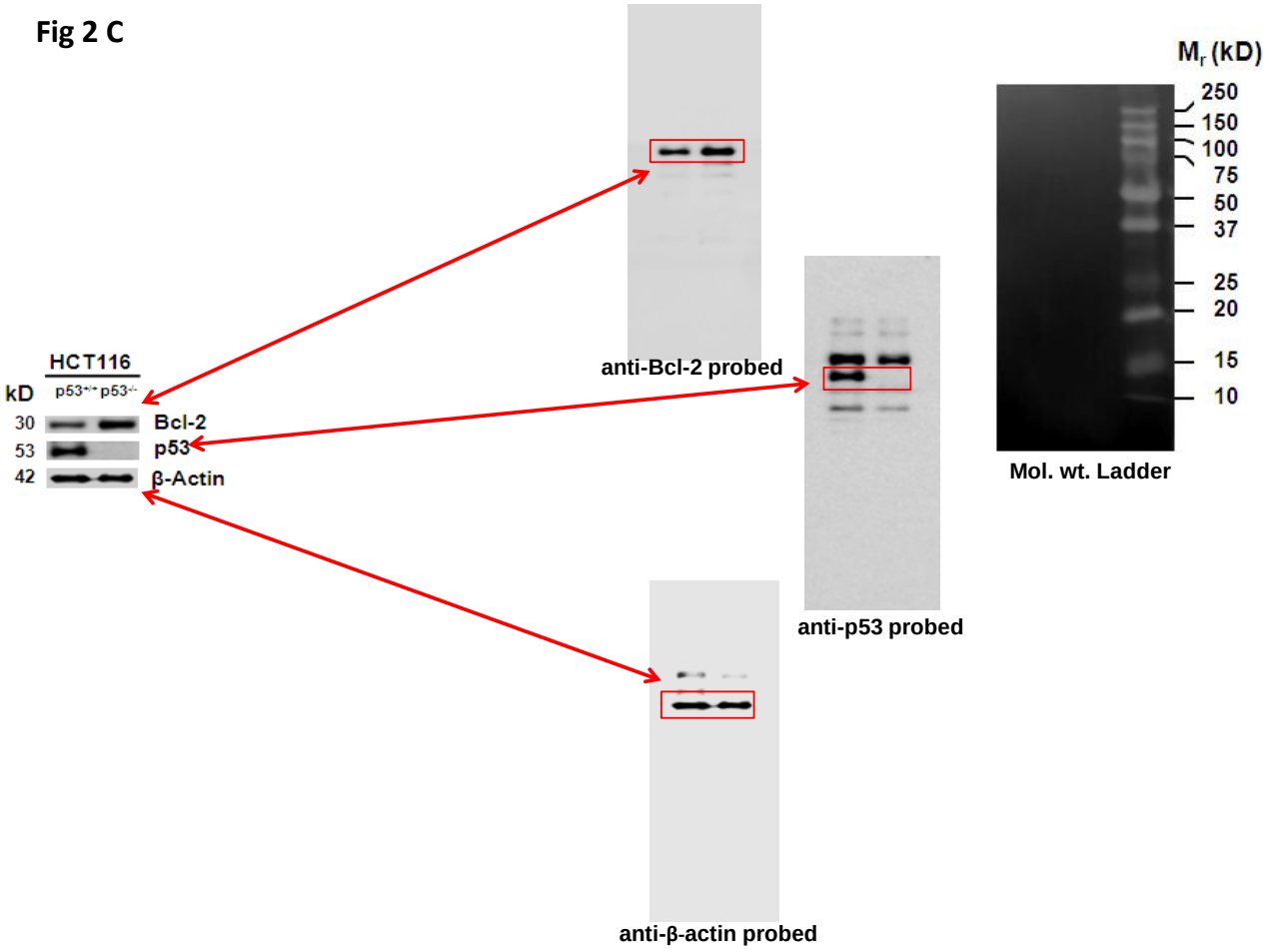

Supplementary Figure 7: Uncropped Western blot images for Fig. 2C

Fig 2 I

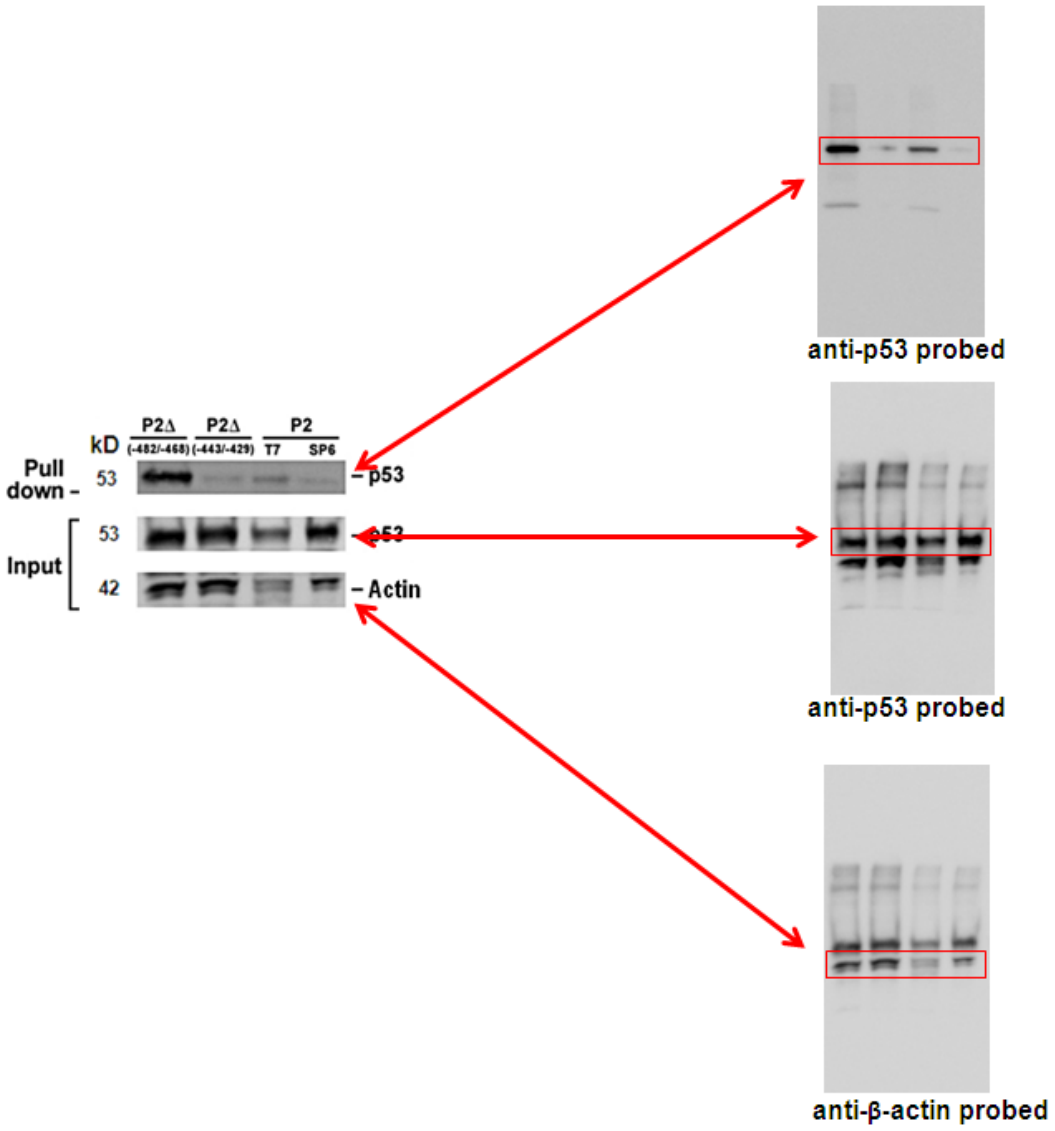

Supplementary Figure 8: Uncropped Western blot images for Fig. 2I

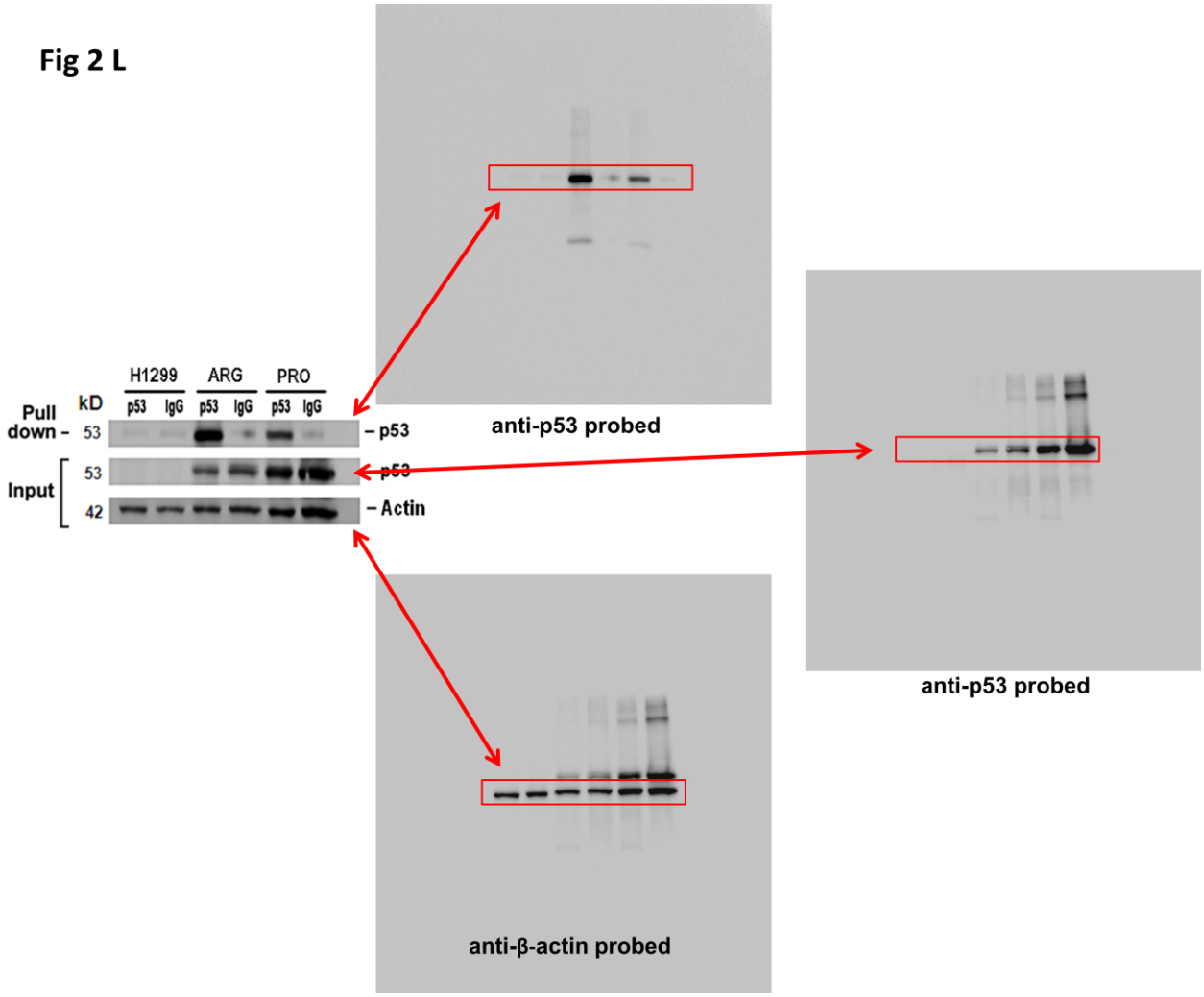

Supplementary Figure 9: Uncropped Western blot images for Fig. 2L

Fig 3C

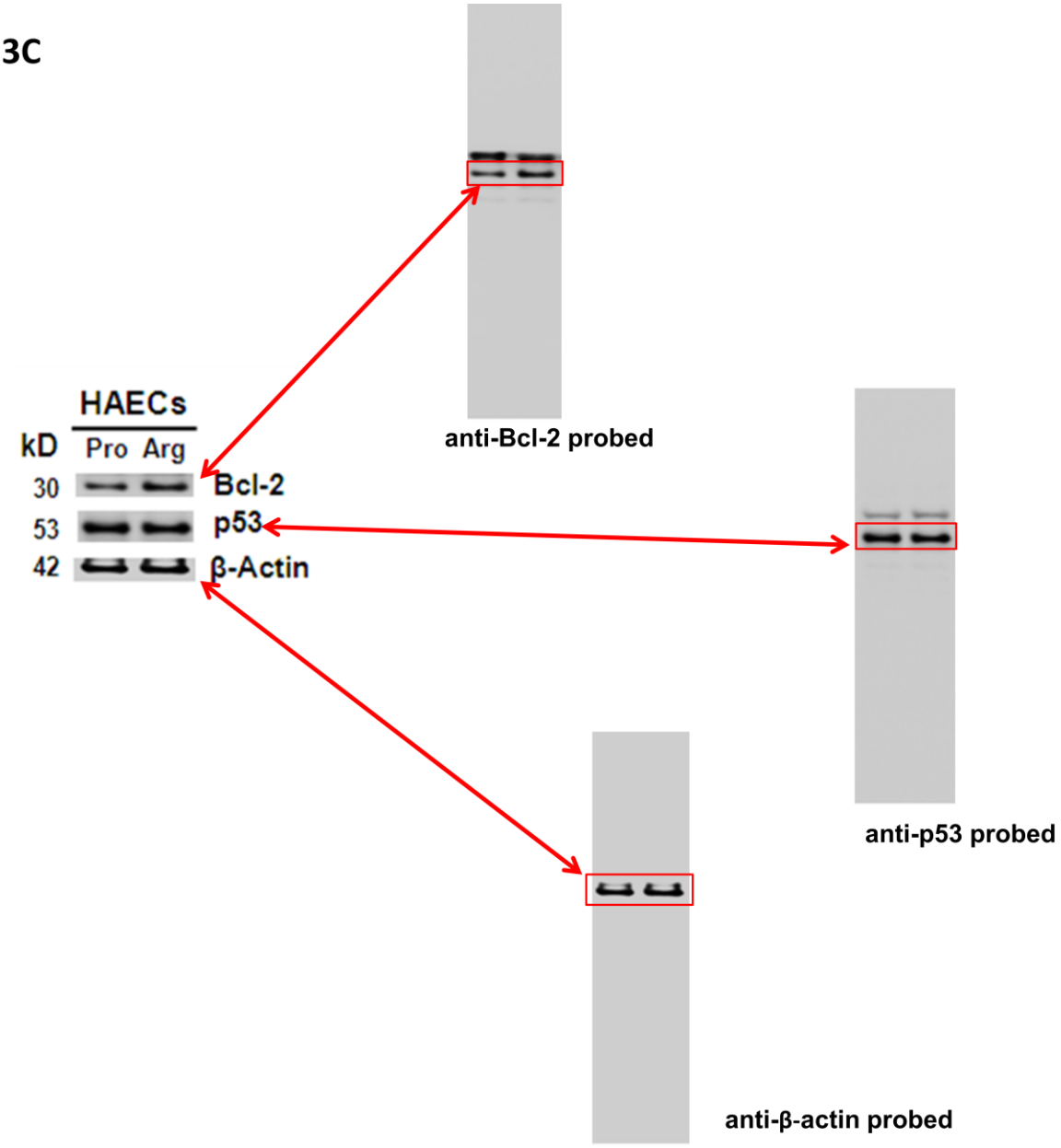

Supplementary Figure 10: Uncropped Western blot images for Fig. 3C

Fig 3H

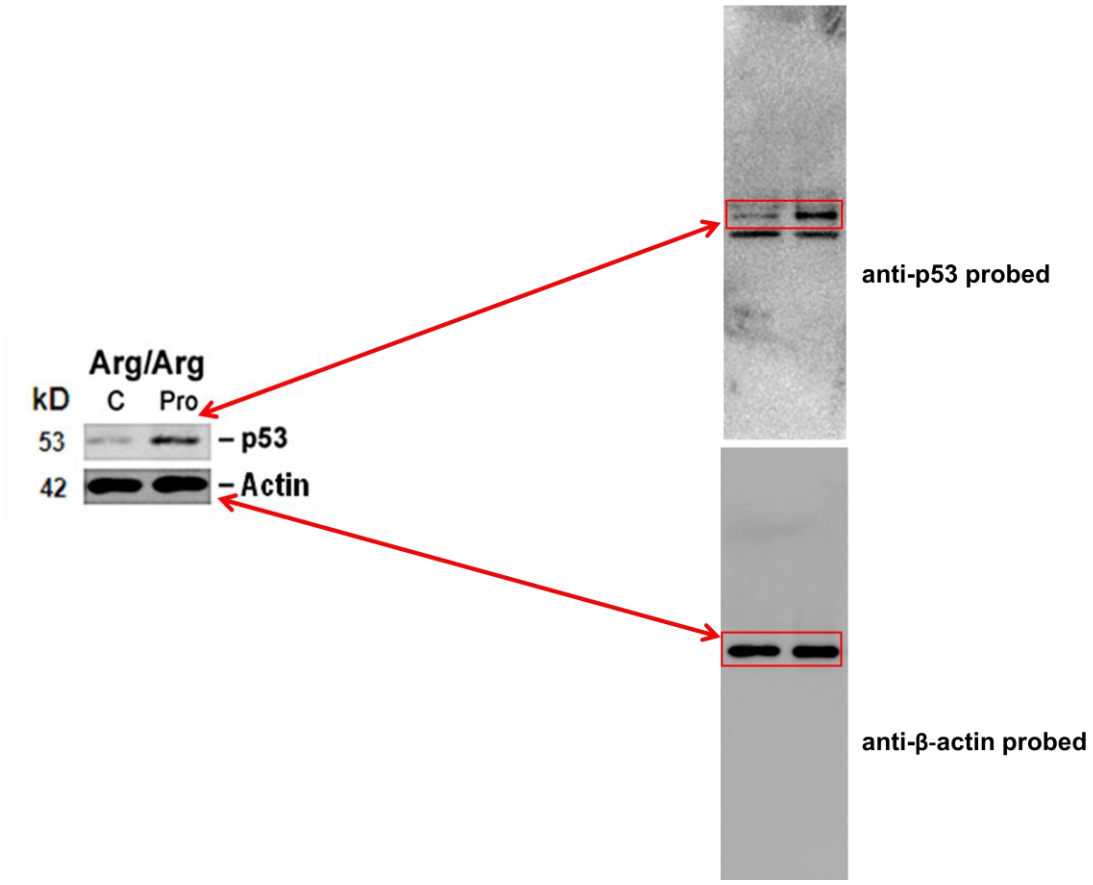

Supplementary Figure 11: Uncropped Western blot images for Fig. 3H

Fig 3 I

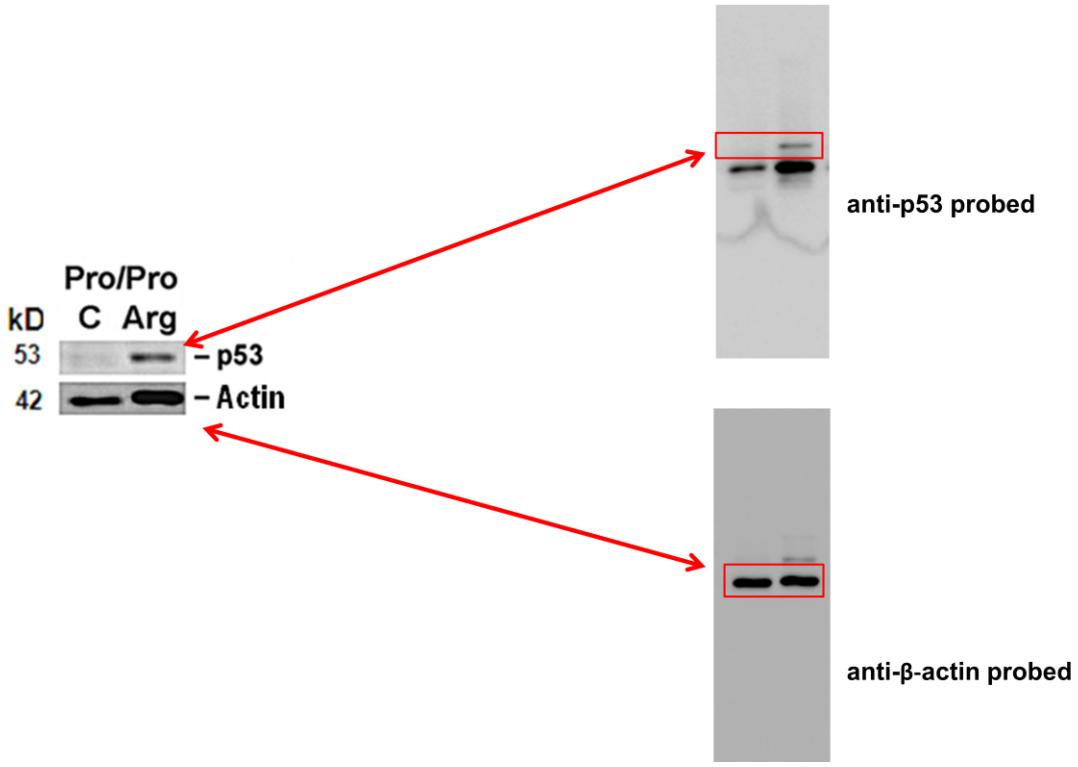

Supplementary Figure 12: Uncropped Western blot images for Fig. 3I

Fig 4 B

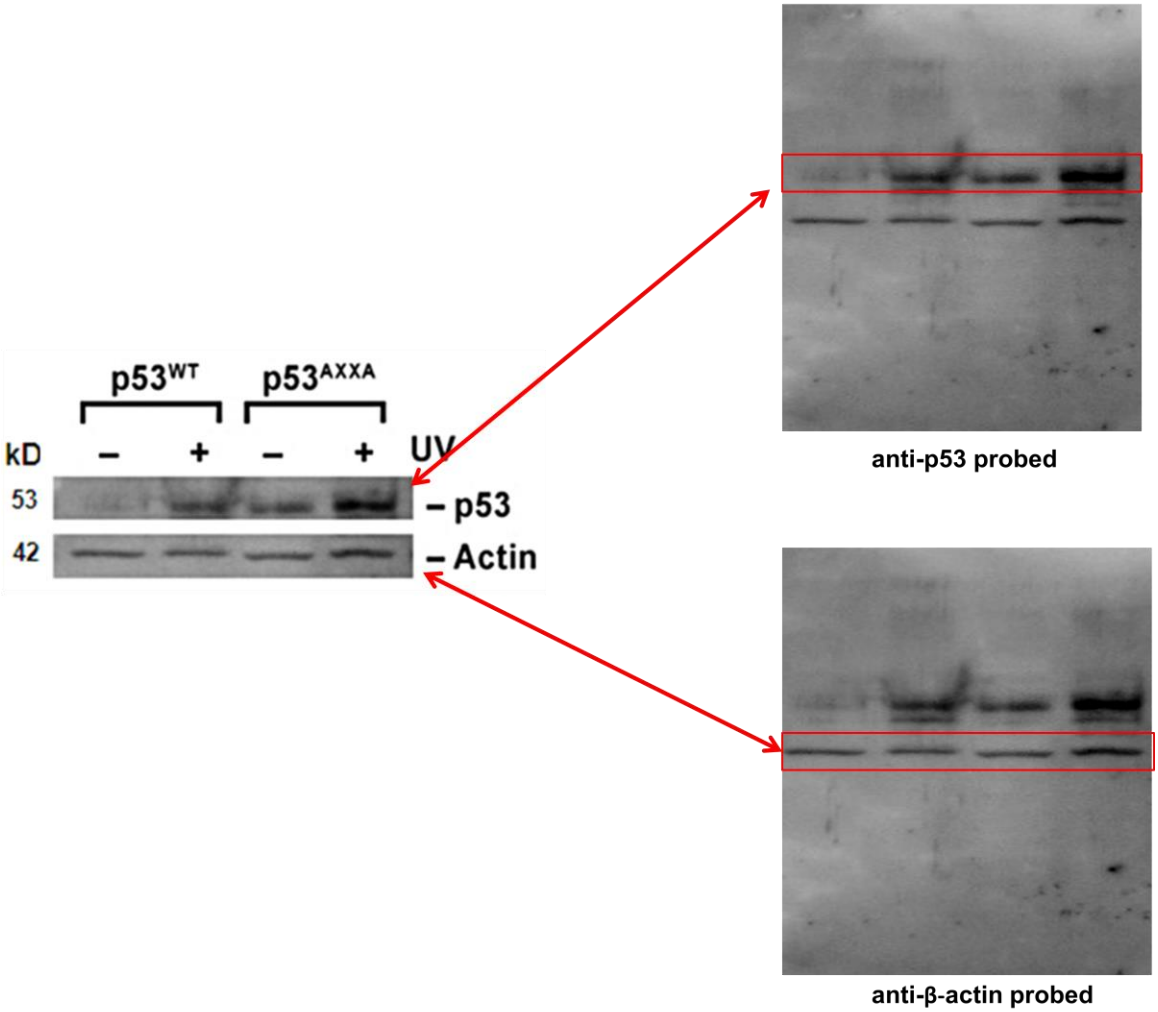

Supplementary Figure 13: Uncropped Western blot images for Fig. 4B

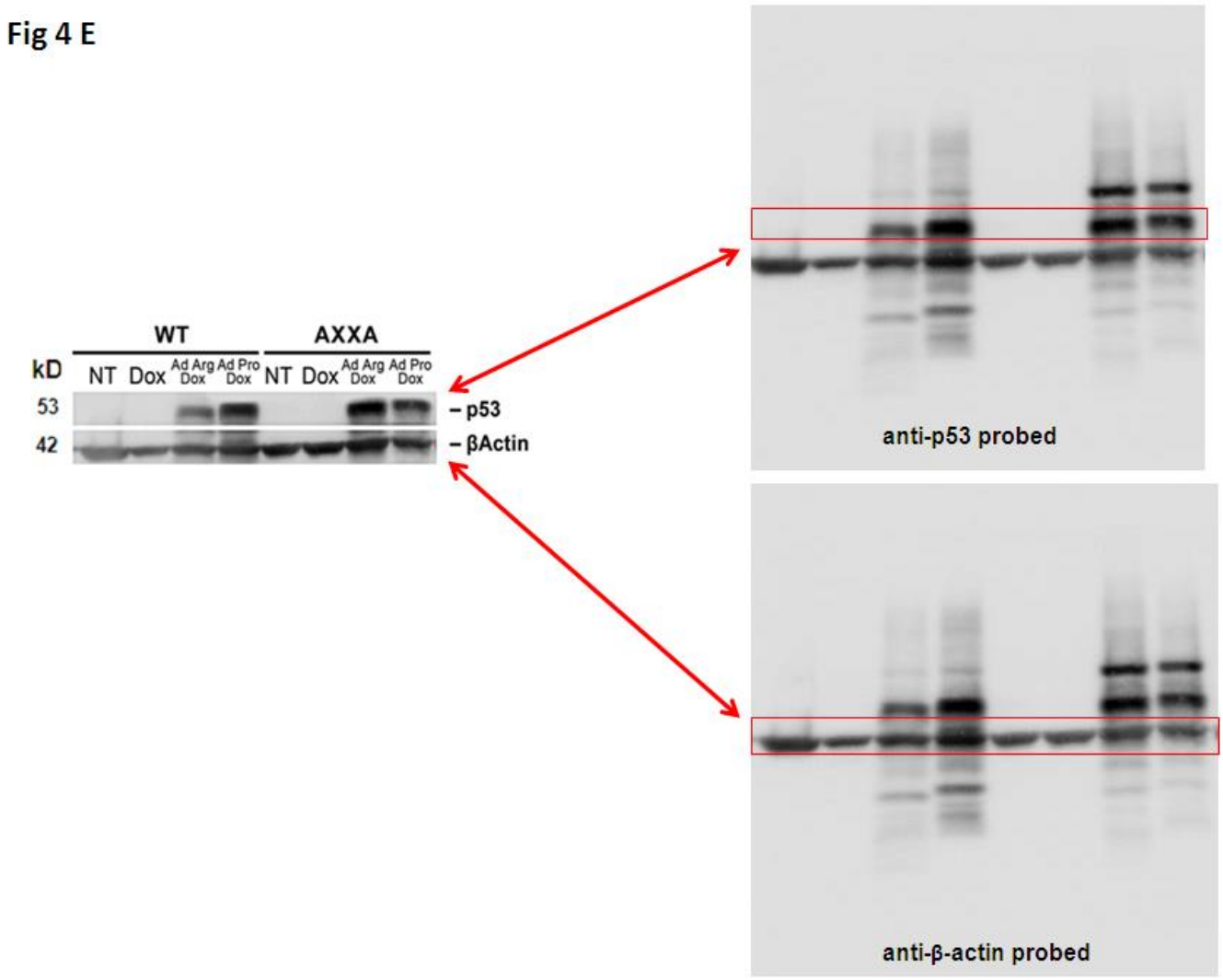

Supplementary Figure 14: Uncropped Western blot images for Fig. 4E

Fig 5C

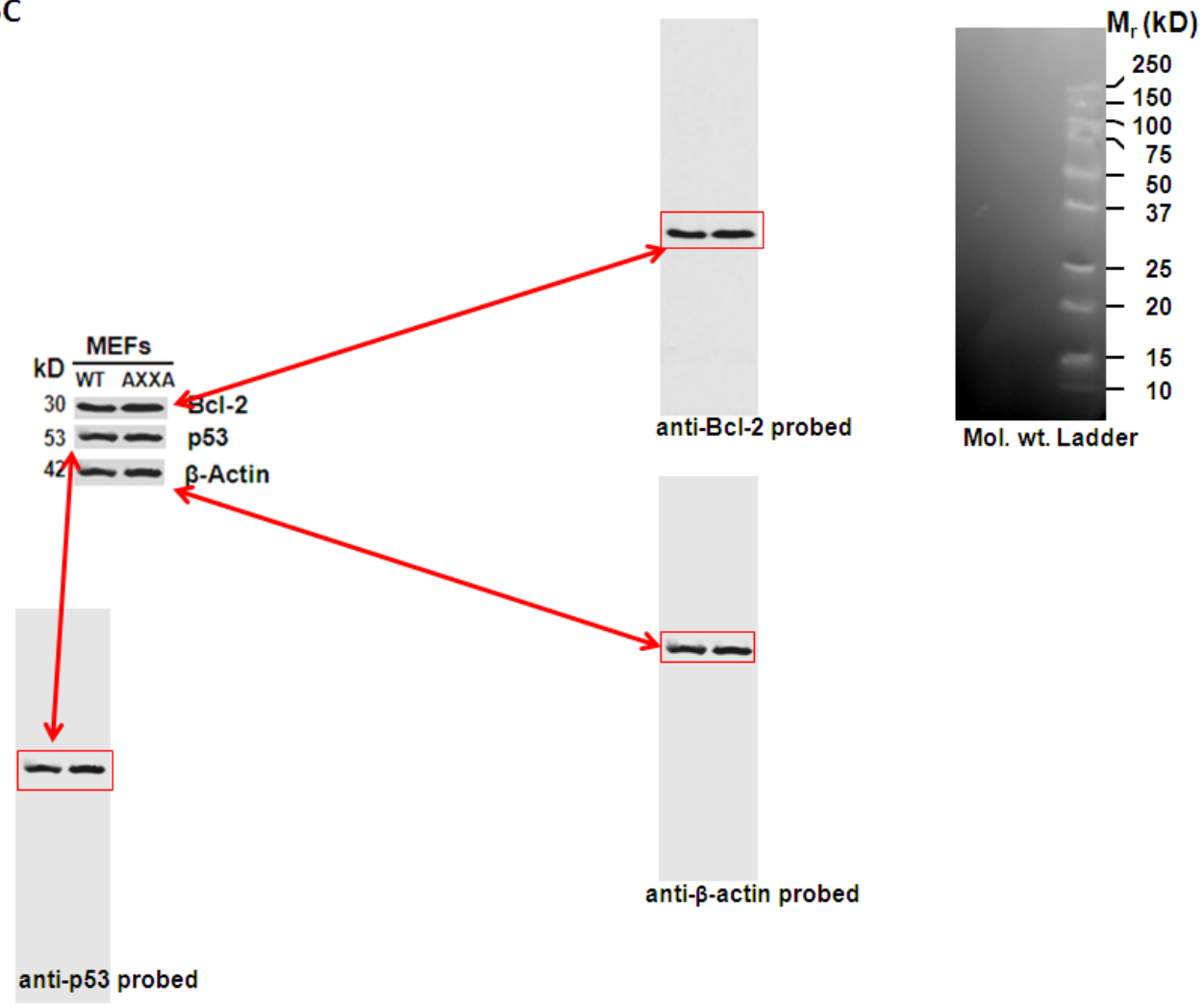

Supplementary Figure 15: Uncropped Western blot images for Fig. 5C

Fig 5F

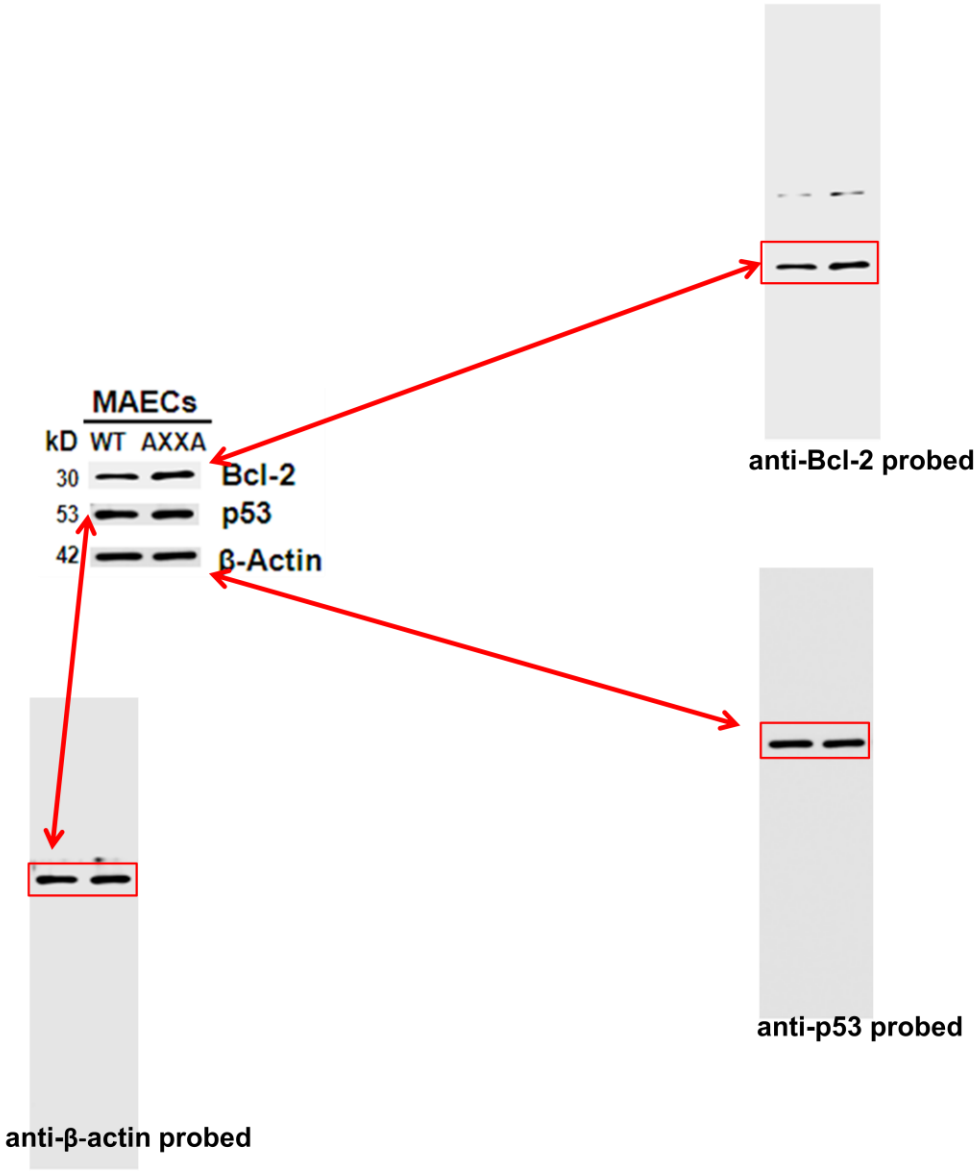

Supplementary Figure 16: Uncropped Western blot images for Fig. 5F

Supplementary Fig 1 C

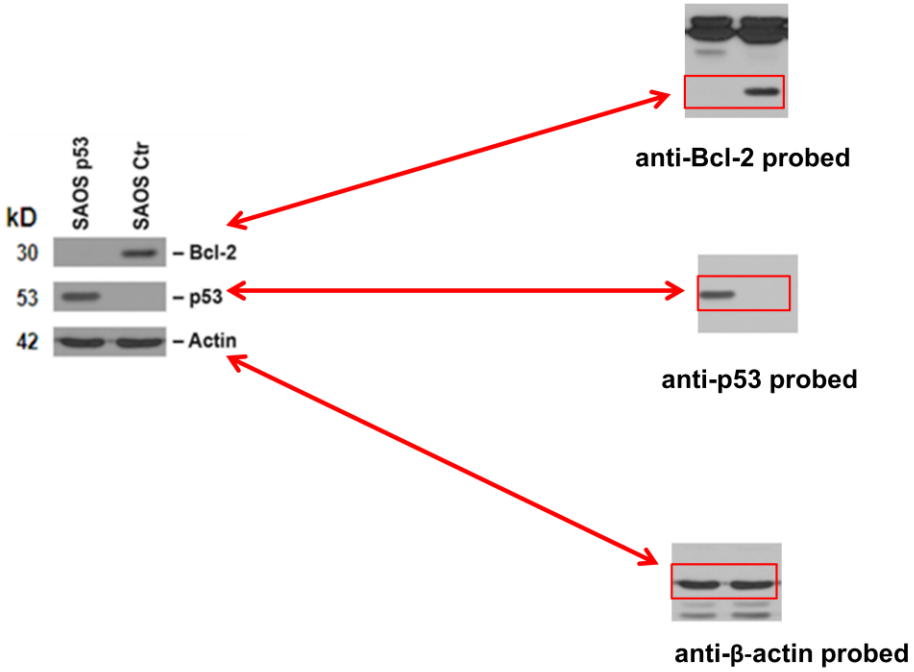

Supplementary Figure 17: Uncropped Western blot images for Supplementary Fig. 1B

Supplementary Fig 4 A

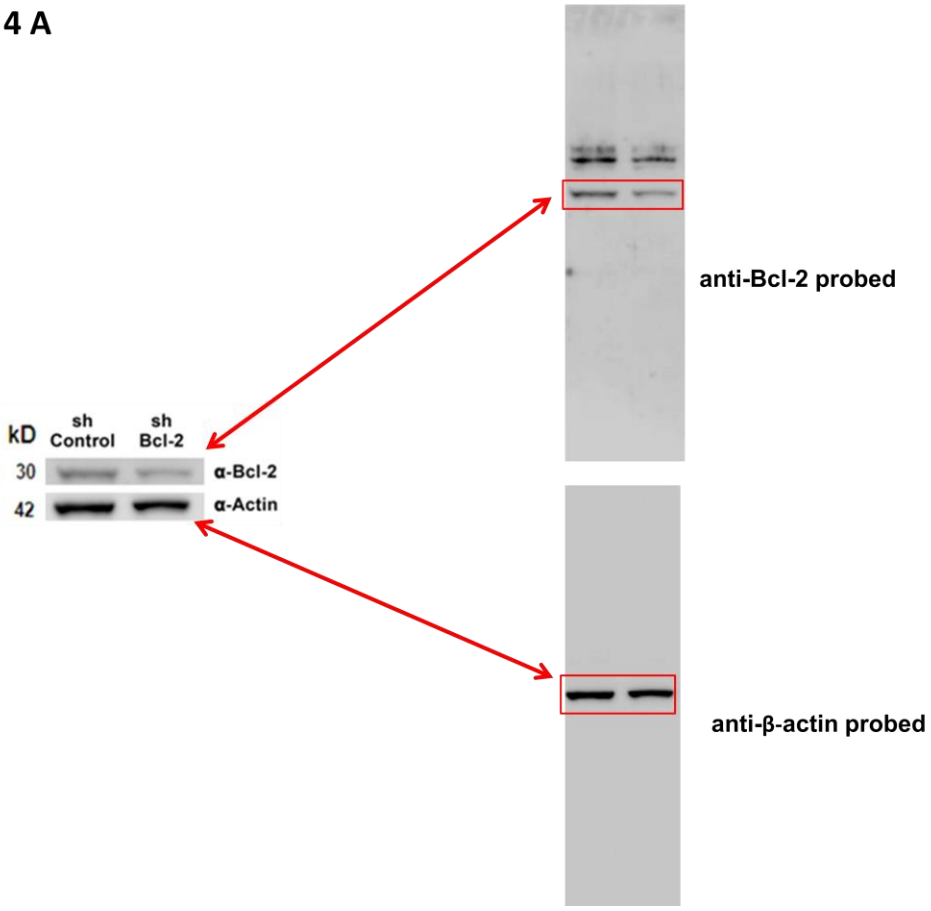

Supplementary Figure 18: Uncropped Western blot images for Supplementary Fig. 4A

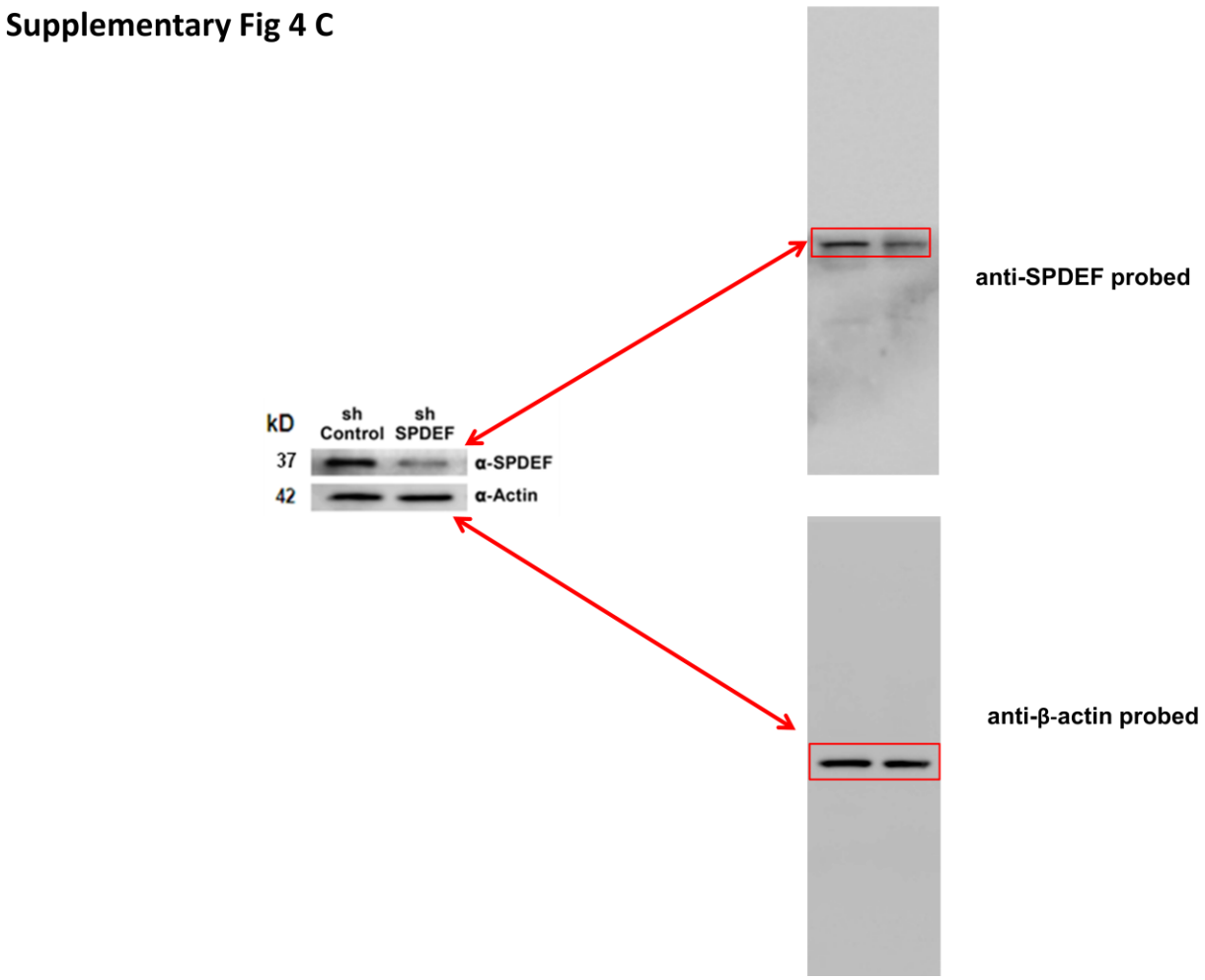

Supplementary Figure 19: Uncropped Western blot images for Supplementary Fig. 4C

Supplementary Table 1: Primers for generation of P2 deletion constructs

Construct	Upstream Primer
Used in all constructs	5'-CTCTTGAGATCTCCGGTTGGGATT-3'

Construct		Downstream Primer
(P1-M-P2Δ1)	-764/-697	5'-GGGAAGCTTTTCTGCTTCACAGAAA-3'
Δ2)	-764/-629	5'-GGGAAGCTTTTCCCAATGAATCAGG-3'
Δ3)	-764/-559	5'-GGGAAGCTTACCAAAACAAATGCAT-3'
Δ4)	-764/-489	5'-GGGAAGCTTTCCTGTGCAGAGAACT-3'
Δ5)	-764/-423	5'-GGGAAGCTTTTTACTCGAATGCACT-3'
Δ6)	-764/-329	5'-GGGAAGCTTCTGAGTGAAAGCAGGG-3'
Δ7)	-764/-277	5'-GGGAAGCTTCTGTGATGCTGAAAGG-3'
Δ8)	-764/-199	5'-GGGAAGCTTTTTATTCCAATTCCTTTCGG-3'
Δ9)	-764/-139	5'-GGGAAGCTTTTTCAATCACGCGGAAC-3'
Δ10)	-764/-69	5'-GGGAAGCTTGAGAAAGAAGAGGAGT-3'

The upstream primer contains a BglII site and all downstream primers contain a HindIII site as underlined.

Supplementary Table 2: Mutations within the 16 nt sequence

Upstream Sequence: GACGTATCTAGATTTTA has the XbaI RE site underlined Downstream Sequence: GTAAAAAGCTTGAATA has the HindIII RE site underlined
16 nucleotide Forward: CTTAAAGTGCATTCGA
Mutant 1 Forward: AGGCCCTGGCATTCGA
Mutant 2 Forward CTTAAAGTTACGGATC
Mutant 3 Forward AGGCAAGTGCATTCGA
Mutant 4 Forward CTTACCTGGCATTCGA
Mutant 5 Forward CTTAAAGTTACGTCGA
Mutant 6 Forward CTTAAAGTGCATGATC
Control Forward GGAGAGTGCTGAAGATTGATGGGATC

Supplementary Table 3: Primers and amplicon sizes for genotypipng of P53 KO, AXXA and TTAA mice

PCR	Forward primer	Reverse Primer	Amplicon (bp)
P53 KO	CTTGGGTGGAGAGGCTATTC	AGGTGAGATGACAGGAGATC	280
P53 WT	ATAGGTCGG CGGTTCAT	CCCGAGTATCTGGAAGACAG	550
P53 AXXA	CAGGAAGCCCAGGTGGAAGCCATAGT	CAAAAAATGGAAGGAAATCAGGAACTAA	300
P53 WT	CAGGAAGCCCAGGTGGAAGCCATAGT	CAAAAAATGGAAGGAAATCAGGAACTAA	400
P53 TTAA	GACGATCTGTTGCTGCCCCAGGATG	TCTAGACAGAGAAAAAAGAGGCATT	200
P53 WT	GACGATCTGTTGCTGCCCCAGGATG	TCTAGACAGAGAAAAAAGAGGCATT	300